JACS
JOURNAL OF THE AMERICAN CHEMICAL SOCIETY
Article
pubs.acs.org/JACS

Mitochondrial Thioredoxin-Responding Off–On Fluorescent Probe

Min Hee Lee,[†,∥] Ji Hye Han,[‡,∥] Jae-Hong Lee,[†] Hyo Gil Choi,[§] Chulhun Kang,*[,‡] and Jong Seung Kim*[,†]

[†]Department of Chemistry, Korea University, Seoul, 136-701, Korea

[‡]The School of East-West Medical Science, Kyung Hee University, Yongin, 446-701, Korea

[§]Protected Horticulture Research Station, National Institute of Horticultural and Herbal Science, Rural Development Administration, Busan, 618-800, Korea

Supporting Information

ABSTRACT: We synthesized a new probe, Mito-Naph, to visualize mitochondrial thioredoxin (Trx) activity in cells. A fluorescence off–on change is induced by disulfide cleavage of the probe, resulting from a reaction with Trx and subsequent intramolecular cyclization by the released thiolate to give a fluorescent product. By measuring the fluorescence at 540 nm, Trx activity can be detected at nanomolar concentrations (down to 50 nM) well below its physiological levels. The in vitro and in vivo Trx preference of Mito-Naph was demonstrated by fluorometric and confocal microscopic experiments. In vitro kinetic analysis of the disulfide bond cleavage revealed that the second-order rate constant for Trx is $(4.04 \pm 0.26) \times 10^3$ $(M\ s)^{-1}$, approximately 5000 times faster than that for GSH. The inhibition experiments involving PX-12, a selective inhibitor of Trx, also revealed that the emission from Mito-Naph significantly decreased in PX-12 dose-dependent manners, both in living cells and in cellular protein extracts. The Trx preference was further supported by an observation that the fluorescence intensity of rat liver extract was decreased according to the Trx depletion by immunoprecipitation. On the basis of these results, it is concluded that Mito-Naph preferentially reacts with Trx, compared with other biological thiols containing amino acids in vitro and in vivo.

INTRODUCTION

Intracellular thiols play essential roles in redox regulation of cell growth, apoptosis inhibition, DNA synthesis, and angiogenesis.[1−3] The major thiols of the redox system are glutathione (GSH) and thioredoxin (Trx).[4,5] Trx is primarily involved in the reducing process of protein disulfides such as ribonucleotide reductase,[6] methionine sulfoxide reductases,[7] and peroxiredoxins.[8] Furthermore, the overexpression of Trx in intracellular and extracellular compartments has been implicated in several types of cancers, cardiovascular diseases, etc.[9−12] In addition, mitochondrial Trx is essential in scavenging oxidatively damaged mitochondrial proteins,[13] regulating mitochondrial permeability transition,[14−16] and participating against apoptosis.[17−19] Moreover, inappropriate levels of mitochondrial Trx are directly associated with mitochondria dysfunctions, resulting in increased reactive oxygen species, higher apoptosis rate, and lower growth.[16,20−23]

Developing sensitive and specific probes toward a thiol is of critical importance for understanding its roles in disease. On discussion of thiol-sensing in biological samples, GSH is always at the center of attention because it is the most abundant thiol in cells.[24] On the other hand, Trx has been mostly overlooked in vivo or in vitro thiol sensing simply because its cellular level seems to be negligible compared to that of GSH (approximately 0.1% of the level of GSH).[25] However, it should be reminded that Trx can catalyze disulfide reduction much faster than dithiothreitol or GSH.[26−28] So, it may be a hasty conclusion that GSH be the most predominant species in the thiol sensing, simply based on its abundance. Accordingly, discussing what is the true target in thiol sensing, the abundance of each thiol and the reactivity for the probe need to be carefully evaluated, which has never been demonstrated in the literatures dealing with thiol sensing so far.

The goal of the present study is to develop a probe able to detect the thiols in mitochondria and to characterize its selectivity on the basis of comparison of the reactivity of Trx with that of GSH, considering their abundances. In particular, the mitochondrial Trx level would be informative in investigating cellular functions related to cancer. This methodology has never been exploited, to the best of our knowledge, and promises to enable researchers to design new drugs in the future.

Here, we report the synthesis and biological application of a fluorescent naphthalimide-based probe (Mito-Naph). It has a mitochondrial guiding moiety and disulfide bond to bring it to the mitochondria and undergo fluorogenic changes upon thiol-catalyzed disulfide bond cleavage.[27,29] The naphthalimide unit provides a suitable fluorescent scaffold owing to its excellent spectroscopic characteristics such as outstanding internal charge transfer (ICT) efficiency, high quantum yield, and structural flexibility for introducing various modifications.[27,30] The triphenylphosphonium headgroup guides it to the mitochondria and also improves its water solubility.[29] The combination of these variations is believed to make in vitro mitochondrial

Received: August 25, 2012
Published: September 27, 2012

dx.doi.org/10.1021/ja308446y | J. Am. Chem. Soc. 2012, 134, 17314−17319

thiol imaging possible in biological and sensory applications.[27,29]

RESULTS AND DISCUSSION

Mito-Naph was prepared by the synthetic route outlined in Scheme 1. The naphthalimide derivatives **1**[31] and **2**[32] were

Scheme 1. Synthetic Route to Mito-Naph

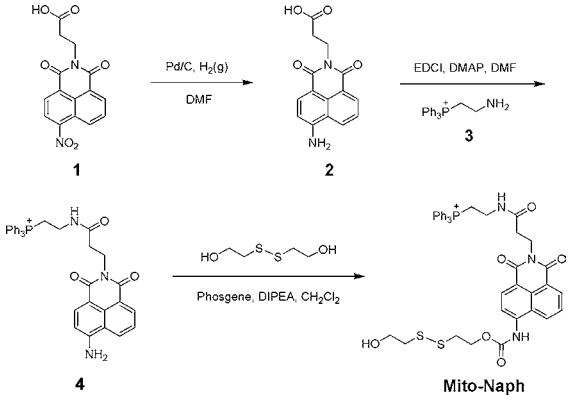

synthesized by adapting published procedures. For the synthesis of **4**, **2** was reacted with **3**[33] in the presence of 1-ethyl-3-(3-(dimethylamino)propyl)carbodiimide (EDCI)/4-(*N*,*N*-dimethylamino)pyridine (DMAP) in DMF. Compound **4** was then reacted with phosgene, followed by treatment with 2,2′-dithiodiethanol, to produce Mito-Naph in 63% yield. To verify the mitochondrial-targeting role of the triphenylphosphonium unit in Mito-Naph, a structural analogue **9** without triphenylphosphonium was also prepared (Supporting Information, Scheme S1). The overall chemical structures of **4** and Mito-Naph were confirmed by ^{1}H NMR, ^{13}C NMR, HR-FAB, and ESI-MS (Supporting Information, Figures S9−S17).

Mito-Naph absorbs and fluoresces at the maxima of 376 and 472 nm, respectively. Upon its addition to a Trx-containing solution under physiological conditions (at 37 °C in PBS buffer, pH 7.4), a new absorption band centered at 428 nm (yellow) and a green emission band at 540 nm appeared concomitantly (Figure 1a,b). The fluorescence spectra at various Trx concentrations are also shown in Figure 1c. With an increasing Trx concentration (0−5.0 μM), the fluorescence intensity at 472 nm decreased, along with the appearance of a new emission band at 540 nm. The spectral change was initiated by disulfide bond cleavage of Mito-Naph by Trx, which in turn was induced by the released thiolate that mounted an intramolecular attack on its amide carbonyl carbon to yield a five-membered carbamate ring and the fluorescent product **4** (Figure 4). We also found a linear correlation between the fluorescence intensity at 540 nm and the Trx concentration (Figure 1d) such that Trx can be detected at nanomolar concentrations (down to 50 nM), below the physiological levels (5−10 μM) of Trx in live cells.[25,34]

Before we attempted to detect Trx in cells with Mito-Naph, interference from other biologically relevant analytes was evaluated under simulated physiological conditions (at 37 °C in PBS buffer of pH 7.4). The fluorescence intensity of Mito-Naph was measured in the presence of amino acids, essential metal ions, or hydrogen peroxide, and the results are depicted in Figure 2. Upon reaction with Trx, the fluorescence of Mito-Naph was enhanced at 540 nm by up to 14 times. In contrast,

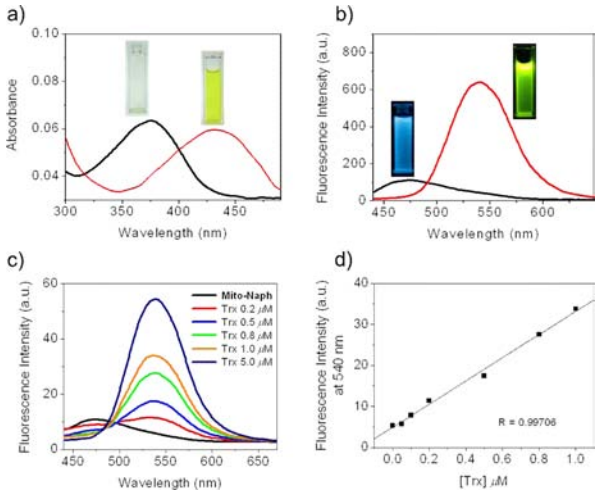

Figure 1. Photophysical changes of Mito-Naph during its reaction with Trx. (a) UV/vis absorption and (b) fluorescence spectra of Mito-Naph (5.0 μM) in the absence (black) and presence (red) of Trx (5.0 μM). (c) Fluorescence changes of Mito-Naph (1.0 μM) with increasing concentrations of Trx (0−5.0 μM). (d) Linear correlation between the fluorescence changes at 540 nm and the Trx concentrations (0−1.0 μM). All spectra were acquired 30 min after Trx addition at 37 °C in PBS buffer (pH 7.4), with excitation λ = 428 nm.

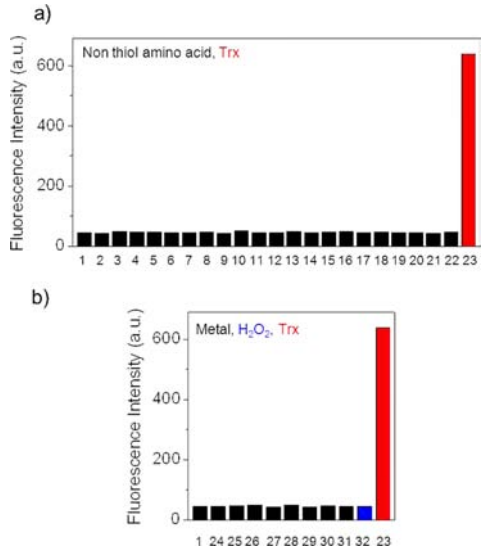

Figure 2. Reactivity of Mito-Naph with Trx in the presence of other putative nonthiol interferants. Fluorescence responses of Mito-Naph (5.0 μM) toward (a) 5.0 mM of nonthiol amino acids (1, only probe; 2, Val; 3, Tyr; 4, Thr; 5, Tau; 6, Ser; 7, Pro; 8, Phe; 9, Met; 10, Lys; 11, Leu; 12, Ile; 13, His; 14, Gly; 15, Gluc; 16, Glu; 17, Gln; 18, Asp; 19, Asn; 20, Arg; 21, Ala; 22, Trp) and 5.0 μM of Trx (23) and (b) 1.0 mM of monovalent metal ions [24, K(I); 25, Na(I)] and 100 μM of di- and trivalent metal ions [26, Ca(II); 27, Cu(II); 28, Fe(II); 29, Fe(III); 30, Mg(II); 31, Zn(II)], and 5.0 mM of H_2O_2 (32). The bars represent the fluorescence intensity at 540 nm. All fluorescence changes were acquired 30 min after the addition of the analytes at 37 °C in PBS buffer (pH 7.4), with an excitation λ = 428 nm.

only an insignificant increase in the emission intensity with other analytes was detected. Furthermore, it should be noted that a new band at 428 nm was apparent in the absorption spectrum only in the presence of Trx (Supporting Information, Figure S1). Together with the data presented in Figure 2, these results demonstrate clearly that reaction of the Mito-Naph with

dx.doi.org/10.1021/ja308446y | J. Am. Chem. Soc. 2012, 134, 17314−17319

Trx is highly favored over other thiols and the accompanying fluorescence enhancement is sufficient to detect cellular Trx pools with negligible interference from other biologically relevant analytes.

In consideration of the preference of Trx for catalyzing disulfide cleavage reactions with Mito-Naph, fluorescence experiments with other biological thiols, such as GSH, cysteine (Cys), and homocysteine (Hcy), were also implemented. The GSH and Trx are known to exist in concentrations of ~10 mM and ~10 μM, respectively, in the human body.[25,34] However, since 10 μM of Trx can be easily oxidized in vitro due to its high activity, the fluorescence changes of Mito-Naph were investigated with 1.0 μM of Trx and 1.0 mM of GSH. As shown in Figures 3 and S2 (Supporting Information), the initial

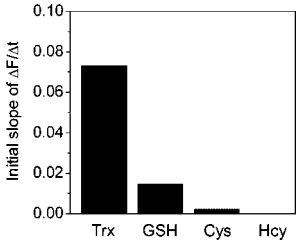

Figure 3. Comparison of the fluorescence enhancement of Mito-Naph in reactions with Trx, GSH, Cys, and Hcy. Fluorescence emission intensities of Mito-Naph (1.0 μM) in the presence of 1.0 μM Trx, 1.0 mM GSH, or 100 μM Cys or Hcy. The bars represent the initial slope of the change in fluorescence intensity at 540 nm as a function of time ($\Delta F/\Delta t$). All fluorescence changes were measured at 37 °C in PBS buffer (pH 7.4), with an excitation λ = 428 nm.

reaction rate ($\Delta F/\Delta t$) in the presence of GSH (1.4×10^{-2}) is slower than that with Trx (7.3×10^{-2}), although GSH (1.0 mM) is more abundant (1000 times) than Trx (1.0 μM). Moreover, only weak or no detectable changes in fluorescence in the presence of 100 μM Cys (2.2×10^{-3}) or Hcy (1.5×10^{-4}) were observed. From these findings, we infer that Mito-Naph shows a selective response to Trx over other thiols, such as GSH, Cys, and Hcy.

To gain insight into the preference of Trx for other thiols, the reaction rate constants were calculated from kinetic analyses of reactions between Mito-Naph and Trx, GSH, Cys, Hcy, or dithiothreitol (DTT). The results are summarized in Table 1,

Table 1. Second-Order Rate Constants for the Reaction of Mito-Naph with GSH, Trx, Cys, Hcy, and DTT

thiols	k^a	$k/k_{GSH}{}^b$
GSH	0.79 ± 0.06	1.00
Trx	(4.04 ± 0.26) × 10^3	5.12 × 10^3
Cys	1.06 ± 0.06	1.06
Hcy	0.58 ± 0.02	0.73
DTT	2.28 ± 0.07	2.88

[a]The second order rate constants are expressed as $(M\ s)^{-1}$. [b]The relative ratio of the rate constants to that of GSH.

and more detailed calculations and plots are shown in Figures S3 and S4 (Supporting Information). We found that the reaction kinetics with Trx, $k = (4.04 \pm 0.26) \times 10^3\ (M\ s)^{-1}$, was approximately 5000 times higher than with GSH. Moreover, the k value for DTT, a strong reducing agent, was much lower [$k = 2.28 \pm 0.07\ (M\ s)^{-1}$].

The dramatic Trx preference of Mito-Naph versus other thiols (Table 1) seems quite unusual considering the fact that the disulfide bond cleavage reaction has been widely used in thiol-mediated sensors[26−28,35−39] or drug delivery systems,[40−42] where it is frequently presumed to occur with GSH or other metabolic thiols such as Cys or Hcy. In contrast, to the best of our knowledge, Trx-mediated disulfide bond cleavage has never been reported in any sensory application yet. To extend our understanding of the basis for the Trx preference in disulfide bond cleavage, a structural analogue possessing a disulfide bond with an ammonium (**7**)[26,35] instead of a hydroxyl end group was also prepared (Scheme S2 and see also Figures S18−S23, Supporting Information), and its kinetic properties were characterized (Supporting Information, Figures S5 and S6). As shown in Table S1 (Supporting Information), similar to the results with Mito-Naph, analogue **7** also shows a much higher rate constant for Trx than for other thiols. Therefore, we firmly conclude that regardless of the end group species, the disulfide bond is preferentially cleaved by Trx, proposing that Trx could contribute to the drug release through the disulfide-mediated drug delivery systems.

To investigate the role of the Cys residues of Trx, the products were analyzed by MALDI-TOF mass spectroscopy. After the reaction with Trx, a peak at m/z 572.0, corresponding to **4**, was predominantly detected (Supporting Information, Figure S8). We also obtained m/z values of 11 611.7 (Trx) and 11 610.3 (Trx-S_2) before and after the reaction, respectively (Supporting Information, Figures S7 and S8). These results confirm that upon reaction with Mito-Naph, Trx was oxidized to yield Trx-S_2 and compound **4** is concomitantly produced (Figure 4). We speculate that the oxidized Trx-S_2 could be reduced by a Trx reductase in cells.

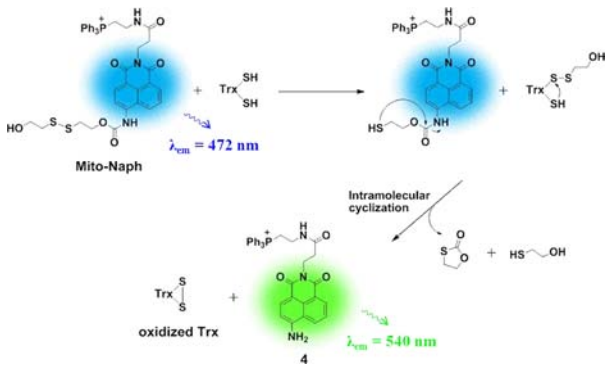

Figure 4. Proposed mechanism of the reaction of Mito-Naph with Trx.

To investigate the contribution of Trx to fluorescence changes generated by Mito-Naph reaction in cells, confocal microscopic observations were performed in the presence of PX-12, a well-known inhibitor of Trx.[43,44] The results (Figures 5a−c) indicate that the fluorescence intensity significantly decreased in a dose (PX-12)-dependent manner (see also Supporting Information, Figure S24). These results also imply that the fluorescence intensity is mainly associated with a Trx-mediated reaction and not with GSH or other metabolic thiols. Moreover, the fluorescence intensity of Mito-Naph in crude cytosolic protein extracts of HepG2 cells reciprocally depends on the concentration of PX-12 (Figure 5d). The removal of Trx by immunoprecipitation (IP) also significantly reduced fluorescence intensity (Figure 5e). From these results, we

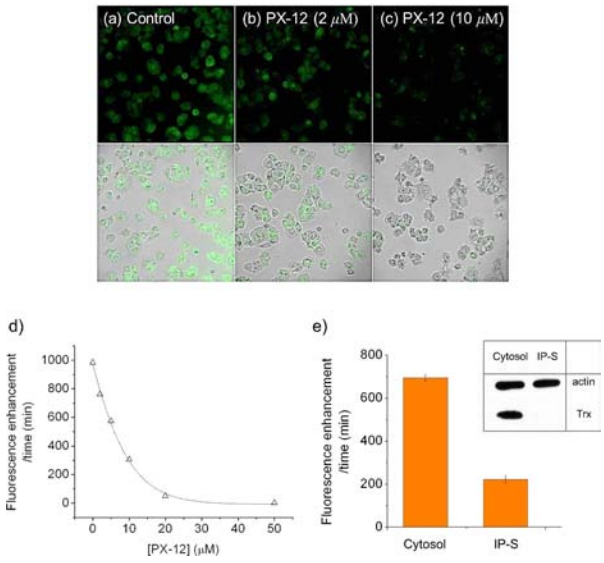

Figure 5. Fluorescence changes of Mito-Naph (5.0 μM) in HepG2 cells and in cytosolic protein extracts. The cells were incubated with media containing PX-12 at (a) 0, (b) 2.0, and (c) 10.0 μM at 37 °C. After 24 h, Mito-Naph was added to each well and incubated for 20 min. Phase contrast (bottom) and fluorescence (top) images were acquired using confocal microscopy at an excitation wavelength of 458 nm and a long path (>505 nm) emission filter. (d) Inhibition of fluorescence intensity of Mito-Naph by PX-12 (0−50 μM) in HepG2 cytosolic protein (1.0 mg/mL, 10 mM of PBS buffer, pH 7.4). (e) Effect of removing Trx by IP on the fluorescence of Mito-Naph (10.0 μM) before (cytosol) and after (IP supernatant). The immunoreactivity of cytosol and IP-S are shown in a Western blot. The excitation and emission wavelengths were 450 and 535 nm, respectively.

firmly conclude herein that the disulfide bond cleavage reaction of Mito-Naph is undergone by Trx in cells.

We also performed the colocalization experiments using Mito-Naph and organelle trackers (Mito-, Lyso-, ER Tracker Red) to determine the location of fluorescence emission. As seen in Figures 6 and S26 (Supporting Information), the fluorescence image of Mito-Naph mainly overlapped with that

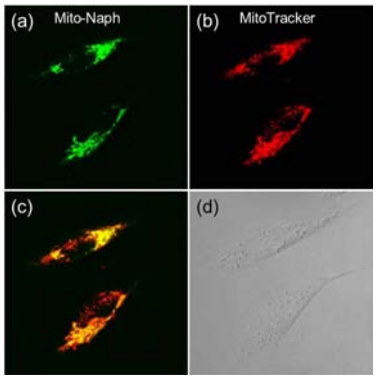

Figure 6. Colocalization experiments using Mito-Naph and MitoTracker Red in HeLa cells. The cells were incubated with 5.0 μM of Mito-Naph for 20 min at 37 °C, and the medium was replaced with fresh medium containing 0.05 μM of MitoTracker Red and incubated for 10 min. Images for Mito-Naph and MitoTracker Red were then obtained using excitation at 458 and 633 nm and band path at (a) 470−600 nm and (b) 650−700 nm, respectively. Panel c is a merged image of panels a and b. Panel d shows phase-contrast image.

of the MitoTracker over other Lyso- or ER Trackers, indicating that Mito-Naph is localized to the mitochondria. In contrast, this type of image overlap was not observed in the case of **9**, where mitochondria-targeting triphenylphosphine is not present (Supporting Information, Figure S25), which is strongly supportive that Mito-Naph reacts mainly with Trx in mitochondria to emit fluorescence.

■ CONCLUSIONS

In conclusion, a new probe bearing naphthalimide, triphenylphosphine, and disulfide moieties has been synthesized, and its photophysical properties and biological application to sensing Trx in a biological environment were examined. We found that the probe can preferentially visualize the activity of Trx in mitochondria, where fluorescence emission is induced by the cleavage of a disulfide bond by the Trx. The colocalization experiments using Mito-Naph and MitoTracker Red demonstrated that Mito-Naph localized to the mitochondria. The in vitro kinetic analysis of disulfide bond cleavage showed that the reaction rate constant for Trx is $(4.04 \pm 0.26) \times 10^3$ $(M\ s)^{-1}$, which means approximately 5000 times faster cleavage than that for the more abundant GSH. The in vivo preference of Mito-Naph for Trx was evident from the confocal microscopic and fluorometric experiments, which revealed that the use of an inhibitor of Trx (PX-12) markedly decreases the intracellular fluorescence in the HepG2 cells and in cell extracts. The preference for Trx was further supported by a concomitant decrease of fluorescence intensity in cell extracts after Trx was depleted by immunoprecipitation. Therefore, Mito-Naph is a mitochondrial Trx probe in cells and could play indispensable roles for understanding the mitochondrial Trx system in vitro and in vivo.

■ EXPERIMENTAL SECTION

Compounds **1**,[31] **2**,[32] **3**,[33] **5**,[26] and **8**[27] were prepared by adapting published procedures.

Synthesis of 4. A mixture of **2** (1.1 g, 3.8 mmol), EDCI (0.74 g, 3.8 mmol), and DMAP (0.47 g, 3.8 mmol) in anhydrous DMF was stirred under nitrogen for 30 min at room temperature. **3** (1.49 g, 3.8 mmol) was then added to the mixture. The reaction mixture was stirred overnight. After removal of solvent, the crude product was purified over silica gel using CH_2Cl_2/MeOH (v/v, 8:2) as the eluent to yield **4** as a orange solid (1.0 g, 68%). ESI-MS: m/z (M^+) calcd 572.2, found 572.3 (M^+). HR-FAB: m/z (M^+) calcd 572.2103, found 572.2103. ^{1}H NMR (CD_3OD, 400 MHz): δ 8.41 (d, 1H, J = 7.3 Hz), 8.33 (d, 1H, J = 7.6 Hz), 8.10 (d, 1H, J = 8.1 Hz), 7.89−7.71 (m, 15H), 7.50 (t, 1H, J = 8.0 Hz), 6.74 (d, 1H, J = 8.2 Hz), 4.33 (t, 2H, J = 7.0 Hz), 3.72−3.47 (m, 4H), 2.48 (t, 2H, J = 7.0 Hz). ^{13}C NMR (CD_3OD, 100 MHz): 173.2, 164.9, 164.2, 153.4, 136.4, 135.2, 133.7, 131.3, 130.3, 129.1, 124.0, 122.1, 119.8, 118.7, 108.4, 108.0, 36.6, 34.6, 33.2, 22.0, 21.5 ppm.

Synthesis of 6. To a mixture of **4** (0.2 g, 0.3 mmol) and phosgene (0.9 mL, 1.7 mmol) in 20 mL of CH_2Cl_2 was added *N*,*N*-diisopropylethylamine (DIPEA) (0.4 mL, 2.4 mmol) dropwise. The resulting solution was stirred for 3 h under nitrogen gas. The reaction mixture was then flushed with nitrogen gas. After unreacted phosgene gas was removed and neutralization occurred in an NaOH bath, synthetic **5** (0.4 g, 1.4 mmol) in CH_2Cl_2 was added to the mixture. The reaction mixture was stirred overnight. The solvent was evaporated off, at which point CH_2Cl_2 (100 mL) and water (100 mL) were added, and the organic layer was collected. The CH_2Cl_2 layer was dried over anhydrous $MgSO_4$. After removal of the solvents, the crude product was purified over silica gel using DCM/MeOH (v/v, 25:2) as the eluent to yield **6** as a yellow solid (0.2 g, 68%). ESI-MS: m/z (M^+) calcd 851.2, found 851.4 (M^+). HR-FAB: m/z (M^+) calcd 851.2702, found 851.2701. ^{1}H NMR ($CDCl_3$, 400 MHz): δ 9.18 (s,

dx.doi.org/10.1021/ja308446y | J. Am. Chem. Soc. 2012, 134, 17314−17319

1H), 9.12 (s, 1H), 8.53 (d, 1H, J = 8.5 Hz), 8.25 (d, 1H, J = 7.6 Hz), 8.04 (d, 1H, J = 8.2 Hz), 7.83−7.69 (m, 15H), 7.46 (t, 1H, J = 7.7 Hz), 5.34 (br s, 1H), 4.50 (t, 2H, J = 6.4 Hz), 4.38 (t, 2H, J = 6.9 Hz), 3.81−3.61 (m, 4H), 3.53−3.43 (m, 2H), 3.04 (t, 2H, J = 6.0 Hz), 2.84 (t, 2H, J = 6.4 Hz), 2.65 (t, 2H, J = 6.8 Hz), 1.41 (s, 9H). ^{13}C NMR ($CDCl_3$, 100 MHz): 172.4, 164.1, 163.6, 156.2, 154.1, 140.3, 135.6, 133.6, 131.9, 131.0, 130.9, 128.8, 126.1, 123.7, 122.5, 118.4, 118.0, 117.5, 79.7, 63.2, 53.7, 38.2, 37.5, 36.9, 34.2, 33.2, 34.2, 33.2, 29.7, 28.6, 22.8, 22.3 ppm.

Synthesis of 7. A solution of TFA/DCM (v/v, 2:1) was added to compound **6** (0.2 g, 0.2 mmol). After 2 h of stirring, the solution was removed under reduced pressure. Diethyl ether was poured in the crude product dissolved in DCM to yield **7** as a yellow solid (0.1 g, 68%). ESI-MS: m/z (M^+) calcd 752.2, found 751.3 ($M - H^+$). HR-FAB: m/z ($M - H^+$) calcd 751.2178, found 751.2178. ^{1}H NMR ($CDCl_3$ with 10% CD_3OD, 400 MHz): δ 8.66 (br s, 1H), 8.49 (d, 1H, J = 9.2 Hz), 8.27 (d, 1H, J = 7.0 Hz), 8.18 (d, 1H, J = 8.3 Hz), 8.05 (d, 1H, J = 8.0 Hz), 7.86−7.66 (m, 15H), 7.49 (t, 1H, J = 7.4 Hz), 4.47 (t, 2H, J = 5.6 Hz), 4.34 (t, 2H, J = 5.8 Hz), 3.58−3.43 (m, 4H), 3.37−3.27 (m, 2H), 3.13−3.01 (m, 4H), 2.57−2.47(m, 2H). ^{13}C NMR ($CDCl_3$ with 10% CD_3OD, 100 MHz): 172.8, 164.4, 163.9, 153.9, 140.5, 135.6, 133.5, 132.2, 131.2, 128.7, 126.3, 123.8, 122.2, 118.3, 117.4, 116.2, 63.2, 38.9, 37.7, 37.1, 34.7, 34.5, 33.5, 22.3, 21.4 ppm.

Synthesis of 9. To a mixture of **8** (0.2 g, 0.7 mmol) and phosgene (0.4 g, 1.4 mmol) in 20 mL of CH_2Cl_2 was added DIPEA (0.5 mL, 2.5 mmol) dropwise. The resulting solution was stirred for 3 h under nitrogen gas. The reaction mixture was flushed with nitrogen gas. After removal of unreacted phosgene gas and neutralization in an NaOH bath, a solution of 2,2′-dithiodiethanol (0.6 g, 3.5 mmol) in CH_2Cl_2/THF (v/v, 1:1) was added to the mixture. The reaction mixture was stirred overnight. The solvent was evaporated off, at which point CH_2Cl_2 (100 mL) and water (100 mL) were added, and the organic layer was collected. The CH_2Cl_2 layer was dried over anhydrous $MgSO_4$. After removal of the solvents, the crude product was purified over silica gel using ethyl acetate/hexane (v/v, 3:2) as the eluent to yield **9** as a yellow solid (0.2 g, 60%). ESI-MS: m/z (M^+) calcd 448.1, found 447.1 ($M - H^+$). HR-FAB: m/z ($M + H^+$) calcd 449.1205, found 449.1204. ^{1}H NMR ($CDCl_3$, 400 MHz): δ 8.61−8.58 (m, 2 H), 8.34 (d, 1H, J = 8.2 Hz), 8.25 (d, 1H, J = 8.5 Hz), 7.62 (br, 1H), 7.75 (t, 1H, J = 8.0 Hz), 4.56 (t, 2H, J = 6.3 Hz), 4.16 (d, 2H, J = 7.5 Hz), 3.96 (t, 2H, J = 5.6 Hz), 3.06 (t, 2H, J = 6.3 Hz), 2.96 (t, 2H, J = 5.8 Hz), 2.40 (br, 1H), 1.74−1.67 (m, 2H), 1.47−1.39 (m, 2H), 0.97 (t, 3H, J = 7.3 Hz). ^{13}C NMR ($CDCl_3$, 100 MHz): 164.3, 163.8, 153.2, 139.0, 132.6, 131.4, 129.1, 126.8, 126.3, 123.6, 123.2, 118.2, 117.2, 64.1, 60.8, 41.7, 40.5, 37.7, 30.4, 20.6, 14.1 ppm.

Synthesis of Mito-Naph. To a mixture of **4** (0.7 g, 1.3 mmol) and phosgene (2.8 mL, 6.5 mmol) in 20 mL of CH_2Cl_2 was added DIPEA (1.4 mL, 9.1 mmol) dropwise. The resulting solution was stirred for 3 h under nitrogen gas. The reaction mixture was then flushed with nitrogen gas. After removal of unreacted phosgene gas and neutralization in an NaOH bath, a solution of 2,2′-dithiodiethanol (0.8 g, 6.5 mmol) in CH_2Cl_2/THF (v/v = 1:1) was added to the mixture. The reaction mixture was stirred overnight. After removal of the solvent, the crude product was purified over silica gel using ethyl CH_2Cl_2/MeOH (v/v, 9:1) as the eluent to yield Mito-Naph as a yellow solid (0.6 g, 63%). ESI-MS: m/z (M^+) calcd 752.2, found 753.5 ($M + H^+$). HR-FAB: m/z (M^+) calcd 752.2018, found 752.2022. ^{1}H NMR ($CDCl_3$, 400 MHz): δ 9.49 (s, 1H), 9.26 (br t, 1H), 8.50 (d, 1H, J = 7.3 Hz), 8.13 (d, 1H, J = 7.6 Hz), 8.07 (d, 1H, J = 8.0 Hz), 7.99 (d, 1H, J = 8.0 Hz), 7.86−7.69 (m, 15H), 7.28 (d, 1H, J = 7.6 Hz), 4.68 (t, 1H, J = 6.0 Hz), 4.50 (t, 2H, J = 6.1 Hz), 4.35 (t, 2H, J = 6.5 Hz), 3.93−3.89 (m, 2H), 3.80−3.75 (m, 2H), 3.69−3.99 (m, 2H), 3.10 (t, 2H, J = 6.2 Hz), 2.99 (t, 2H, J = 6.3 Hz), 2.73 (t, 2H, J = 7.1 Hz). ^{13}C NMR ($CDCl_3$, 100 MHz): 172.7, 164.1, 163.6, 154.2, 140.6, 135.6, 133.6, 131.9, 130.9, 130.8, 128.8, 128.4, 126.0, 123.4, 122.0, 118.4, 117.6, 116.9, 63.6, 60.6, 41.7, 38.0, 37.1, 34.4, 33.4, 22.6, 22.9 ppm.

Synthetic Materials and Methods. All reactions were carried out under nitrogen atmosphere. All reagents, including thioredoxin (from *Escherichia coli*), amino acids, metal ions, thiols, and other chemicals for synthesis, were purchased from Aldrich and used as received. Mito Tracker Red is purchased from Molecular Probes (Invitrogen). All solvents were HPLC reagent grade, and triple-deionized water was used throughout the analytical experiments. Silica gel 60 (Merck, 0.063−0.2 mm) was used for column chromatography. Analytical thin layer chromatography was performed using Merck 60 F254 silica gel (precoated sheets, 0.25 mm thick). ^{1}H and ^{13}C NMR spectra were collected in $CDCl_3$ or CD_3OD (Cambridge Isotope Laboratories, Cambridge, MA) on Varian 300 and 400 MHz spectrometers. ESI mass spectrometric analyses were carried out using an LC/MS-2020 Series (Shimadzu) instrument. HR-FAB mass spectral analyses were carried out at Korea Basic Science Institute.

UV/Vis and Fluorescence Spectroscopy. Stock solutions of Mito-Naph, **7**, and biologically relevant analytes, including Trx, GSH, Cys, Hcy, Val, Tyr, Thr, Tau, Ser, Pro, Phe, Met, Lys, Leu, Ile, His, Gly, Gluc, Glu, Gln, Asp, Asn, Arg, Ala, Na(I), K(I), Zn(II), Mg(II), Fe(III), Fe(II), Cu(II) and Ca(II), were prepared in triple-distilled water. Absorption spectra were recorded on an S-3100 (Scinco) spectrophotometer, and fluorescence spectra were recorded using an RF-5301 PC spectrofluorometer (Shimadzu) equipped with a xenon lamp. Samples for absorption and emission measurements were contained in quartz cuvettes (3 mL volume). Excitation was provided at 428 nm with excitation and emission slit widths at 3 nm. All spectroscopic measurements were performed under physiological conditions (at 37 °C in PBS buffer, pH 7.4).

Kinetic Data. Kinetic measurements were performed using a Shimadzu RF-5301PC spectrometer in single-mixing mode by mixing the two reactants. The time dependences of the response of Mito-Naph (1.0 μM) or **7** (1.0 μM) to thiols (GSH, Trx, Cys, Hcy, and DTT) were determined at 540 nm, with a time interval of 0.16 s. In the case of Trx, reduced Trx was prepared by incubating 50 μM Trx with 250 μM DTT for 1 h at 37 °C. Excitation was performed at 428 nm, with all excitation and emission slit widths at 3 nm. All kinetic measurements were performed under physiological conditions (at 37 °C in PBS buffer, pH 7.4).

Cell Culture. A human hepatoma cell line (HepG2) and a human cervical cancer cell line (HeLa) were cultured in Dulbecco's modified Eagle's medium (DMEM) supplemented with 10% fetal calf serum, 1% penicillin, and 10 000 units/mL of streptomycin at 37 °C, under humidified air containing 5% CO_2; 1 $\times 10^5$ cells per well were plated on a 24-well plate. Cell images were obtained using a confocal microscope from Carl Zeiss (LSM 510 META model). Other information is available in the figure captions.

Immunoprecipitation. Cells were homogenized in homogenization buffer (320 mM sucrose, 4.0 mM HEPES, 1.0 mM EDTA, and 100 mM DTT, pH 7.4), and homogenates were centrifuged at 10 000g for 10 min at 4 °C. The pellet was removed, and the crude cytosol was collected. The collected crude cytosol was treated with anti-Trx antibody (Abcam) overnight at 4 °C and further incubated with anti-antibody Protein G PLUS-Agarose (Santa Cruz Biotechnology) overnight. The agarose beads were pelleted by centrifugation (1000g for 5 min), and the Trx-depleted supernatant was collected and immediately used for Trx activity assay.

Western Blot. Thirty mircograms of protein per sample was loaded per well on 12% polyacrylamide gels. After electrophoresis was performed, the separated proteins were transferred onto nitrocellulose membranes (Bio-Rad, Hercules, CA) in transfer buffer [39 mM glycine, 48 mM Tris-base, pH 8.3, 0.37% (w/v) SDS, 20% (v/v) methanol]. Membranes were blocked with 5% nonfat dried milk in TBS-T buffer [20 mM Trix-base, pH 7.6, 137 mM NaCl, 0.1% (v/v) Tween-20] for 1 h at room temperature. Membranes were then incubated with anti-Trx antibody (Abcam) overnight at 4 °C and further incubated with HRP-conjugated anti-antibody (Santa Cruz Biotechnology) for 1 h. Anti-β-actin (Sigma-Aldrich) was used to establish the internal standard. The blots were washed three times with TBS-T buffer, and the immune-reactive protein bands were visualized by application of ECL substrate solution (INTRON Biotechnology).

■ ASSOCIATED CONTENT

Supporting Information

Additional spectra (UV/vis absorption, fluorescence, NMR, ESI-MS) and imaging data and full reference information. This material is available free of charge via the Internet at http://pubs.acs.org.

■ AUTHOR INFORMATION

Corresponding Author

kangch@khu.ac.kr; jongskim@korea.ac.kr

Author Contributions

‖These authors contributed equally to the work.

Notes

The authors declare no competing financial interest.

■ ACKNOWLEDGMENTS

This work was supported by the CRI project (20120000243) of the National Research Foundation of Korea (J.S.K.) and the Cooperative Research Program for Agriculture Science & Technology Development (Project No. PJ008959), Rural Development Administration, Republic of Korea (C.K.).

■ REFERENCES

(1) Dalton, T. P.; Shertzer, H. G.; Puga, A. *Annu. Rev. Pharmacol. Toxicol.* **1999**, *39*, 67−101.

(2) Zhang, S. Y.; Ong, C. N.; Shen, H. M. *Cancer Lett.* **2004**, *208*, 143−153.

(3) Herzenberg, L. A.; De Rosa, S. C.; Dubs, J. G.; Roederer, M.; Anderson, M. T.; Ela, S. W.; Deresinski, S. C.; Herzenberg, L. A. *Proc. Natl. Acad. Sci. U. S. A.* **1997**, *94*, 1967−1972.

(4) Arnér, E. S. J.; Holmgren, A. *Eur. J. Biochem.* **2000**, *267*, 6102−6109.

(5) Bindolia, A.; Rigobello, M. P.; Scutari, G.; Gabbiani, C.; Casini, A.; Messori, L. *Coord. Chem. Rev.* **2009**, *253*, 1692−1707.

(6) Holmgren, A. *Annu. Rev. Biochem.* **1985**, *54*, 237−271.

(7) Holmgren, A.; Johansson, C.; Berndt, C.; Loenn, M. E.; Hudemann, C.; Lillig, C. H. *Biochem. Soc. Trans.* **2005**, *33*, 1375−1377.

(8) Haendeler, J.; Hoffmann, J.; Tischler, V.; Berk, B. C.; Zeiher, A. M.; Dimmeler, S. *Nat. Cell Biol.* **2002**, *4*, 743−749.

(9) Yamada, Y.; Nakamura, H.; Adachi, T.; Sannohe, S.; Oyamada, H.; Kayaba, H.; Yodoi, J.; Chihara, J. *Immunol. Lett.* **2003**, *86*, 199−205.

(10) Yoshida, S.; Katoh, T.; Tetsuka, T.; Uno, K.; Matsui, N.; Okamoto, T. *J. Immunol.* **1999**, *163*, 351−358.

(11) Kumagai, S. *Rinsho Byori* **1998**, *46*, 574−580.

(12) Lincoln, D. T.; Ali Emadi, E. M.; Tonissen, K. F.; Clarke, F. M. *Anticancer Res.* **2003**, *23*, 2425−2433.

(13) Patenaude, A.; Ven Murthy, M. R.; Mirault, M.-E. *J. Biol. Chem.* **2004**, *279*, 27302−27314.

(14) He, M.; Cai, J.; Go, Y.-M.; Johnson, J. M.; Martin, W. D.; Hansen, J. M.; Jones, D. P. *Toxicol. Sci.* **2008**, *105*, 44−50.

(15) Wang, D.; Masutani, H.; Oka, S.-I.; Tanaka, T.; Yamaguchi-Iwai, Y.; Nakamura, H.; Yodoi, J. *J. Biol. Chem.* **2006**, *281*, 7384−7391.

(16) Damdimopoulos, A. E.; Miranda-Vizuete, A.; Pelto-Huikko, M.; Gustafsson, J. A.; Spyrou, G. *J. Biol. Chem.* **2002**, *277*, 33249−33257.

(17) Saitoh, M.; Nishitoh, H.; Fujii, M.; Takeda, K.; Tobiume, K.; Sawada, Y.; Kawabata, M.; Miyazono, K.; Ichijo, H. *EMBO J.* **1998**, *17*, 2596−2606.

(18) Tanaka, T.; Hosoi, F.; Yamaguchi-Iwai, Y.; Nakamura, H.; Masutani, H.; Ueda, S.; Nishiyama, A.; Takeda, S.; Wada, H.; Spyrou, G.; Yodoi, J. *EMBO J.* **2002**, *21*, 1695−1703.

(19) Saxena, G.; Chen, J.; Shalev, A. *J. Biol. Chem.* **2009**, *285*, 3997−4005.

(20) Nonn, L.; Williams, R. R.; Erickson, R. P.; Powis, G. *Mol. Cell. Biol.* **2003**, *23*, 916−922.

(21) Zhou, R.; Tardivel, A.; Thorens, B.; Choi, I.; Tschopp, J. *Nat. Immunol.* **2010**, *11*, 136−140.

(22) Karlenius, T. C.; Tonissen, K. F. *Cancers* **2010**, *2*, 209−232.

(23) Behl, C.; Davis, J. B.; Lesley, R.; Schubert, D. *Cell* **1994**, *77*, 817−827.

(24) Hwang, C.; Sinskey, A. J.; Lodish, H. F. *Science* **1992**, *257*, 1496−1502.

(25) Bhat, G. B.; Iwase, L.; Hummel, B. C. W.; Walfish, P. G. *Biochem. J.* **1989**, *258*, 785−792.

(26) Pires, M. M.; Chmielewski, J. *Org. Lett.* **2008**, *10*, 837−840.

(27) Lee, M. H.; Han, J. H.; Kwon, P.-S.; Bhuniya, S.; Kim, J. Y.; Sessler, J. L.; Kang, C.; Kim, J. S. *J. Am. Chem. Soc.* **2012**, *134*, 1316−1322.

(28) Chen, X.; Zhou, Y.; Peng, X.; Yoon, J. *Chem. Soc. Rev.* **2010**, *39*, 2120−2135.

(29) Robinson, K. M.; Janes, M. S.; Pehar, M.; Monette, J. S.; Ross, M. F.; Hagen, T. M.; Murphy, M. P.; Beckman, J. S. *Proc. Natl. Acad. Sci. U. S. A.* **2006**, *103*, 15038−15043.

(30) Zhang, J. F.; Zhou, Y.; Yoon, J.; Kim, J. S. *Chem. Soc. Rev.* **2011**, *40*, 3416−3429.

(31) Patrick, L. G. F.; Whiting, A. *Dyes Pigm.* **2002**, *55*, 123−132.

(32) Yuan, D.; Brown, R. G.; Hepworth, J. D.; Alexiou, M. S.; Tyman, J. H. P. *J. Heterocycl. Chem.* **2008**, *45*, 397−404.

(33) Maryanoff, B. E.; Reitz, A. B.; Duhl-Emswiler, B. A. *J. Am. Chem. Soc.* **1985**, *107*, 217−226.

(34) Powis, G.; Mustacich, D.; Coon, A. *Free Radical Biol. Med.* **2000**, *29*, 312−322.

(35) Lee, J. H.; Lim, C. S.; Tian, Y. S.; Han, J. H.; Cho, B. R. *J. Am. Chem. Soc.* **2010**, *132*, 1216−1217.

(36) Pullela, P. K.; Chiku, T.; Carvan, M. J.; Sem, D. S. *Anal. Biochem.* **2006**, *352*, 265−273.

(37) Piggott, A. M.; Karuso, P. *Anal. Chem.* **2007**, *79*, 8769−8773.

(38) Zhu, B.; Zhang, X.; Li, Y.; Wang, P.; Zhang, H.; Zhuang, X. *Chem. Commun.* **2010**, *46*, 5710−5712.

(39) Liu, C.; Pan, J.; Li, S.; Zhao, Y.; Wu, L. Y.; Berkman, C. E.; Whorton, A. R.; Xian, M. *Angew. Chem., Int. Ed.* **2011**, *50*, 10327−10329.

(40) Santra, S.; Kaittanis, C.; Santiesteban, O. J.; Perez, J. M. *J. Am. Chem. Soc.* **2011**, *133*, 16680−16688.

(41) Kim, E.; Kim, D.; Jung, H.; Lee, J.; Paul, S.; Selvapalam, N.; Yang, Y.; Lim, N.; Park, C. G.; Kim, K. *Angew. Chem., Int. Ed.* **2010**, *49*, 4405−4408.

(42) El Alaoui, A.; Schmidt, F.; Amessou, M.; Sarr, M.; Decaudin, D.; Florent, J.-C.; Johannes, L. *Angew. Chem., Int. Ed.* **2007**, *46*, 6469−6472.

(43) Kirkpatrick, D. L.; Kuperus, M.; Dowdeswell, M.; Potier, N.; Donald, L. J.; Kunkel, M.; Berggren, M.; Angulo, M.; Powis, G. *Biochem. Pharmacol.* **1998**, *55*, 987−994.

(44) Welsh, S. J.; Williams, R. R.; Birmingham, A.; Newman, D. J.; Kirkpatrick, D. L.; Powis, G. *Mol. Cancer Ther.* **2003**, *2*, 235−243.